
1 **Experimental investigation on an integrated thermal management system**
2 **with heat pipe heat exchanger for electric vehicle**

3 Huiming Zou^a, Wei Wang^c, Guiying Zhang^{a,b}, Fei Qin^{a,b}, Changqing Tian^a,
4 Yuying Yan^d

5 a.Beijing Key Laboratory of Thermal Science and Technology and Key Laboratory of Cryogenics,
6 Technical Institute of Physics and Chemistry, CAS, Beijing 100190, P. R. China,
7 zouhuiming@mail.ipc.ac.cn

8 b.University of Chinese Academy of Sciences, Beijing, China

9 c.China FAQ Group Corporation R&D Center, Changchun, China

10 d.HVACR & Heat Transfer Research Group, Faculty of Engineering, University of Nottingham,
11 U.K.

12
13 **Abstract:**

14 An integrated thermal management system combining a heat pipe battery
15 cooling/preheating system with the heat pump air conditioning system is presented to
16 fulfill the comprehensive energy utilization for electric vehicles. A test bench with
17 battery heat pipe heat exchanger (HPHE) and heat pump air conditioning for a regular
18 five-chair electric car is set up to research the performance of this integrated system
19 under different working conditions. The investigation results show that as the system
20 is designed to meet the basic cabinet cooling demand, the additional parallel branch of
21 battery chiller is a good way to solve the battery group cooling problem, which can
22 supply about 20% additional cooling capacity without input power increase. Its
23 coefficient of performance(COP) for cabinet heating is around 1.34 at -20°C out-car
24 temperature and 20°C in-car temperature. The specific heat of the battery group is
25 tested about 1.24 kJ/kg·°C. There exists a necessary temperature condition for the
26 HPHE to start action. The heat pipe heat transfer performance is around 0.87 W/°C

27 on cooling mode and $1.11 \text{ W/}^\circ\text{C}$ on preheating mode. The gravity role makes the heat
28 transfer performance of the heat pipe on preheating mode better than that on cooling
29 mode.

30

31 **Key words:** Electric vehicles, Heat pump, Heat pipe, Battery temperature control,
32 Thermal management

33 **Nomenclature:**

34 A_{hp} contact superficial area with coolant of each heat pipe (m^2)

35 c_b specific heat of battery group ($\text{kJ/kg}^\circ\text{C}$)

36 c_c specific heat of coolant ($\text{kJ/kg}^\circ\text{C}$)

37 m_b mass of battery group (kg)

38 m_c mass of coolant (kg)

39 n heat pipe number

40 Q_{bi} batteries internal heat variation (kW)

41 Q_c cooling capacity by battery chiller (kW)

42 Q_{ci} coolant internal heat variation (kW)

43 Q_g generated heat by batteries (kW)

44 Q_p preheating heat by PTC (kW)

45 Q_t transferred heat by HPHE (kW)

46 q_{hp} heat transfer coefficient of each heat pipe ($\text{W/}^\circ\text{C}$)

47 T_{ba} average temperature of battery group ($^\circ\text{C}$)

48	T_{bo}	coolant outlet temperature ($^{\circ}\text{C}$)
49	T_{bi}	coolant inlet temperature ($^{\circ}\text{C}$)
50	T_{ca}	coolant average temperature ($^{\circ}\text{C}$)
51	ΔT	average temperature difference between the battery group and the coolant ($^{\circ}\text{C}$)
52	t	time (s)

53 **1. Introduction**

54 Electric vehicle (EV) is an important development orientation to alleviate the
55 traditional automobile exhaust problem. However, thermal management including
56 battery temperature control and cabinet air conditioning is a big challenge for EV, as
57 the traditional engine and oil tank are replaced by electric motor and battery groups.

58 Lots of heat inside of the battery generated by the electrochemical reaction will
59 raise the battery temperature up sharply, affect its working efficiency badly and even
60 cause safety problem [1, 2]. Sato[3] analyzed the thermal behavior of lithium-ion
61 batteries showing that when the battery temperature was over 50°C , charging
62 efficiency and life cycle would be considerably diminished. Khateeb et al. [4] pointed
63 out that the safety of the Li-ion battery would descend when it operated at the
64 temperature range of $70\text{-}100^{\circ}\text{C}$. Studies have shown that there is a necessary
65 temperature range for battery to make sure its performance and service life. Pesaran [5]
66 presented that the best range of operating temperature for batteries such as lead-acid,
67 NiMH, and Li-ion are from 25 to 40°C and suitable temperature distribution from
68 module to module is below 50°C . To control the batteries in the suitable temperature

69 range, there are several methods presented [6-12], such as by air directly, by liquid
70 with plate heat exchanger or by refrigerant phase change with plate or pipe heat
71 exchanger. However, investigations on the thermal behavior of batteries [5,13-14]
72 show that the relationship between the generated heat and discharge rate is nonlinear
73 direct ratio and the higher the discharge rate is, the quicker the increase rate of the
74 generated heat will be. While the discharge rate changes with the working conditions
75 such as acceleration, deceleration, uphill, and downhill. So generated heat of the
76 battery is variable and its instantaneous value is very high. This means the cooling
77 capacity of the battery temperature control system with these normal methods has to
78 be set high enough to avoid the battery on extremely high temperature and lead to an
79 over-size thermal management system. Therefore it is very significant to search for a
80 more efficient battery heat-transfer method to simplify the EV thermal management
81 system.

82 Heat pipe, as a high efficient heat-transfer device combining the principles of
83 both thermal conductivity and phase transition, is a novel idea to apply on the
84 temperature control of EV battery [15]. Actually, because of its highly effective
85 thermal conductivity, heat pipe has been applied successfully in many fields such as
86 electron cooling, solar heater and energy recovering [16, 17]. As for the above
87 mentioned EV battery thermal characteristics, heat pipes between the batteries can
88 help transfer the heat out to the coolant so that the batteries can be maintained in the
89 best operating temperature range under variable working conditions and the

90 temperature difference between batteries can be eliminated [18]. Moreover, because
91 the coolant system has enough thermal capacity, the cooling load can be much lower
92 than that of the instant cooling method. It just needs to meet the average heat
93 dissipation demand instead of the peak generated heat during high discharge rate
94 conditions. Therefore, heat pipe is a promising development orientation for batteries
95 thermal management of EV. Authors' initial investigations have shown that the heat
96 pipe cooling is an effective method [19]. However, the previous study results were
97 mainly concentrating on the basic thermal performance of a single heat pipe unit with
98 a simple experimental apparatus. The thermal performance of the heat pipe heat
99 exchanger (HPHE) for the practical EV battery group still has not been researched,
100 which might be different from that of the single heat pipe because of cluster effect.

101 On the other hand, since EV has no engine to drive compressor for cooling and
102 no waste engine heat for heating, heat pump system with motor-driven compressor is
103 an important development trend. The investigation on the performance of heat pump
104 system has become a major topic of EV air-conditioning. Suzuki and Katsuya [20]
105 proposed a heat pump system for electric vehicle with functions of cooling, heating,
106 demisting and dehumidifying and their experimental results showed the feasibility of
107 heat pump. However, heat pump system has a shortcoming that its heating capacity
108 drops sharply with the decreasing outdoor temperature. Hosoz and Direk [21, 22]
109 indicated this feature by investigating the performance of R134a heat pump system
110 transformed for the original automobile air conditioning system. In recent years many

111 advances on heat pump system for EV have been presented [23]. Authors [24, 25]
112 have also engaged in the heat pump performance improvement with injection
113 technology and got notable achievement in system heating capacity and COP under
114 extremely cold condition. However when it comes to practical performance of the
115 heat pump system combining with battery temperature control system, there is few
116 literature either.

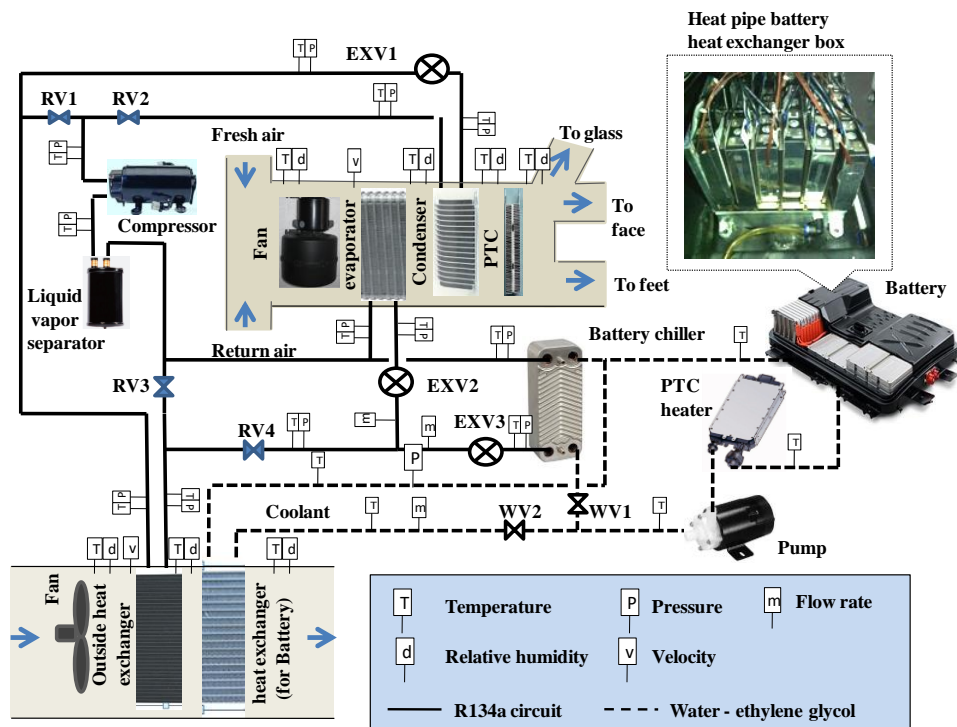
117 In this paper, an integrated thermal management system combining a HPHE for
118 battery cooling/preheating with a heat pump air conditioning is presented to
119 investigate its performance characteristics on different working conditions. Cooling
120 and heating performances of the system, as well as the thermal performance of HPHE,
121 are investigated by bench test, hoping to present a significative reference for the EV
122 thermal management.

123 **2. System description and experimental bench setup**

124 2.1 System description

125 Fig.1 shows the diagram of the heat pump coupling with battery cooling
126 /preheating system based on regular five-chair electric cars and takes R134a as
127 refrigerant. Its working temperature ranges from -20°C to 45°C . The heat pump system
128 mainly consists of a variable-frequency scroll compressor, an outside heat exchanger
129 with a fan, a liquid vapour separator, four refrigerant valves (RV), a condenser
130 followed by an expansion valve (EXV1) for cabinet heating, an refrigerant-air

131 evaporator following with EXV2 for cabinet cooling and a refrigerant-water
 132 evaporator for battery cooling called battery chiller. The refrigerant-air evaporator and
 133 condenser are installed in the ventilation duct. The system is switched by the RVs for
 134 cooling or heating. The battery cooling/preheating system also applies a water-air heat
 135 exchanger in front of the car to utilize the natural cooling source and a Positive
 136 Temperature Coefficient (PTC) heater to preheat the battery in cold season. A HPHE
 137 is installed among the battery group, called battery heat exchanger box here. Please
 138 refer the reference [20] for more details of the HPHE.



139

140

Fig.1. Diagram of the heat pump coupling with the battery cooling/preheating system

141 2.2 Experimental bench

142 Correspondingly a test bench is set up inside of a psychrometer testing room to

143 investigate the performance of this system. The experiments are carried out on

144 cooling and heating mode respectively under different working conditions. On
 145 cooling mode, the refrigerant valve RV1 and RV4 are open while RV2 and RV3 are
 146 closed. The opening of expansion valves EXV2 and EXV3 are changed repeatedly to
 147 get the optimum branch refrigerant flow rate of the cabin evaporator and battery
 148 chiller. On heating mode, the refrigerant valve RV1 and RV4 are closed while RV2
 149 and RV3 are open. The battery is preheated by the PTC heater. The coolant pipe
 150 system and battery heat exchanger box are isolated to prevent unmeasured heat loss.
 151 There are 30 real battery modules in the bench for electric cars, but the generated heat
 152 during discharging process is simulated by electric films for the sake of safety. The
 153 electric films are pasted on the two wide sides of each battery module and
 154 thermocouples are pasted on the other two narrow sides to measure the temperature
 155 response of the batteries. Each side has three thermocouples. The measurement
 156 devices of the bench are shown in Fig.1 and their parameters are shown in Table 1.
 157 The relative parameters of the bench are shown in Table 2.

158 Table 1 Measurement devices

Parameter	Type	Range	Error
Temperature	Thermocouple	-30 to 220°C	±0.5°C
Pressure	Diaphragm	0 to 30bar	±0.5%
Air speed	Hot bulb	0 to 40m/s	±3%
Mass flow rate of Ref.	Coriolis	<370kg/h	±0.1%

159
160 Table 2 Parameter of the bench

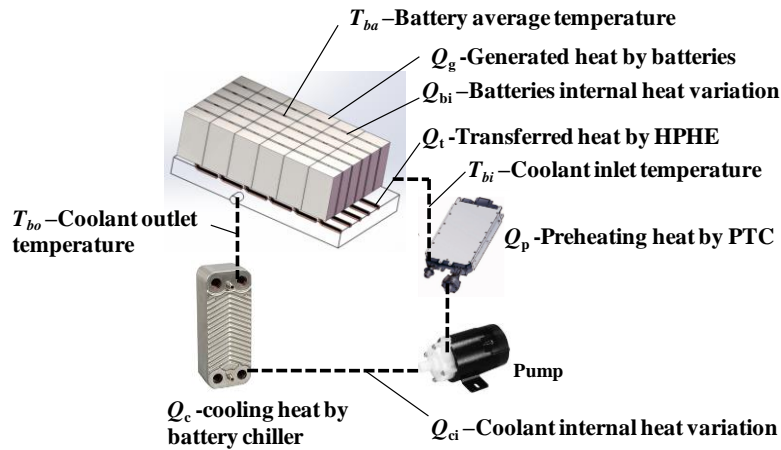
Item	Symbol	Value(unit)
------	--------	-------------

Mass of battery group	m_b	16.03 kg
Mass of coolant	m_c	3.96 kg
Specific heat of ethylene glycol coolant	c_c	3.334 kJ/kg°C @ -20°C
		3.518 kJ/kg°C @ 35°C
Contact superficial area with coolant of each heat pipe	A_{hp}	3.552 kJ/kg°C @ 45°C
		0.00188 m ²
Heat pipe number	n	25

161

162 2.3 Calculation methodology

163 To investigate the heat transfer performance of HPHE of battery group, the
 164 experiment is carried out to simulate different working modes. The heat composition
 165 of the battery temperature control system is shown as Fig.2. The battery internal heat
 166 variation and coolant internal heat variation can be expressed as equation (1) and (2)
 167 respectively. Here heat transfer coefficient of each heat pipe q_{hp} is applied to indicate
 168 the heat transfer performance of the HPHE, which can be expressed as equation(3).



169

170

Fig.2 Heat composition of the battery group temperature control system

171

$$Q_{bi} = c_b m_b \frac{dT_{ba}}{dt} = Q_g + Q_t \quad (1)$$

$$Q_{ci} = c_c m_c \frac{dT_{ca}}{dt} = Q_t + Q_p + Q_c \quad (2)$$

$$q_{hp} = \frac{Q_t}{n\Delta T} \quad (3)$$

Because the system heat-transfer process goes from dynamic to steady state gradually and the energy during the initial dynamic process is not balanced, it is important to note that this model is only suitable for the final steady state.

3. Experimental result and discussion

3.1 Heat pump system performance

Table 3 shows the system cooling and heating performance under different working conditions.

Table 3 Cooling/heating performance of the heat pump system

Experiment No.	1	2	3	4	5	6
Out-car temperature (°C)	35	35	45	45	-20	-20
In-car temperature (°C)	27	27	45	45	-20	20
EXV1 opening (%)	0	0	0	0	100	100
EXV2 opening (%)	84	84	63	63	0	0
EXV3 opening (%)	0	40	0	90	0	0
Evaporator evaporating temperature (°C)	-1.49	-0.48	9.96	11.7	-23.13	-21.58
Super-heating temperature (°C)	0.93	0.76	1.28	2.59	0.01	1.37
Battery chiller evaporating temperature (°C)	--	-4.30	--	7.49	--	--
Super-heating temperature (°C)	--	18.35	--	0.36	--	--
Condensing temperature (°C)	41.18	41.58	55.4	54.31	20.78	58
Sub-cooling temperature (°C)	0.3	0	7.36	1.98	21.62	9.45
Cabinet refrigerant flow rate (kg/h)	135.16	134.0	192.01	180.4	43.2	47.56
Cabinet cooling/heating capacity (kW)	5.24	5.19	7.22	6.61	2.96	2.75
Battery chiller refrigerant flow rate (kg/h)	--	25.36	--	63.96	--	--

Battery chiller cooling capacity (kW)	--	1.09	--	2.31	--	--
Theoretical compression power (kW)	1.04	1.24	1.43	1.75	0.45	0.86
Actual input power (kW)	2.44	2.46	3.13	3.19	1.48	2.04
Compression efficiency (%)	42.51	50.34	45.53	55.0	30.27	42.05
COP	2.15	2.55	2.31	2.80	2.0	1.34

182

183 On cooling mode under out-car 35°C and in-car 27°C condition, the opening of
184 EXV1 is kept on 84% while that of EXV3 is changed from 0 to 40%. The evaporator
185 cooling capacity decreases lightly and the battery chiller cooling capacity increases
186 quickly. The total cooling capacity increases about 19.84% and the compressor input
187 power almost keeps the same, so the system COP increases about 18.60%. Under
188 out-car 45°C and in-car 45°C condition, the optimum opening of EXV2 is 63% and
189 that of EXV3 is 90%. And also the system total cooling capacity and COP under this
190 conditions are both increases. Compare to the out-car 35°C and in-car 27°C
191 condition, the cooling capacity for both cabin and battery as well as system COP are
192 much higher because of the lower compression ratio under this condition. The
193 experimental results of cooling performance show that the additional parallel branch
194 of battery chiller is a good way to solve the battery cooling problem, which can
195 supply about 20% additional cooling capacity without input power increase.

196 On heating mode under out-car -20°C and in-car -20°C condition, system
197 condensing temperature is about 20°C. As the in-car temperature increases to 20°C,
198 system condensing temperature increases to 58°C, heating capacity decreases from

199 2.96 kW to 2.75kW, the compressor input power increases from 1.48 kW to 2.04 kW,
200 and the heating COP decreases from 2.0 to 1.34. The experimental results show that
201 although the heating COP under -20°C in-car temperature is higher than that under
202 20°C because of the lower compression ratio, the compression efficiency of the scroll
203 compressor is much lower. This is because the motor efficiency of scroll compressor
204 drops rapidly under lower load conditions. The heating capacity is insufficient for
205 the cabinet heating. Therefore PTC heater is suggested to be an auxiliary heat source
206 under extremely cold weather.

207

208 3.2 Heat pipe heat exchanger performance

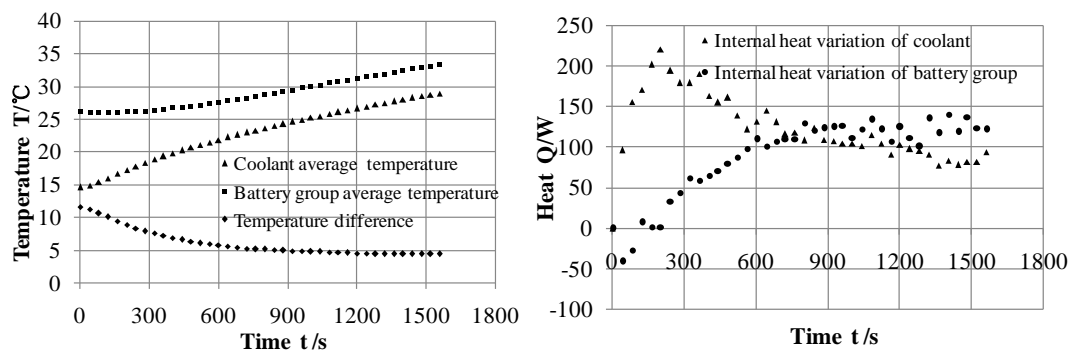
209 3.2.1 Testing mode without heating or cooling

210 Because the battery group is a composition of electrolyte, metal and heat pipe etc.,
211 and the thermal capacity characteristics of different material are different, the specific
212 heat of battery group is uncertain. A testing experiment is carried out firstly to test the
213 specific heat of battery group. On this mode, the coolant is circulated by the pump
214 with neither PTC heating nor battery chiller cooling and the generated heat of battery
215 group is dissipated to the coolant by the HPHE. The equation (1) and (2) can be
216 transferred into equation (4).

$$217 \quad c_b m_b \frac{dT_{ba}}{dt} = Q_g - c_c m_c \frac{dT_{ca}}{dt} \quad (4)$$

218 Fig.3(a) shows the average temperature response tendency of the battery group
219 and the coolant from start to steady state. The temperature difference between them
220 decreases from 11.6°C to a constant 4.4°C. Fig.3(b) shows the internal heat variation

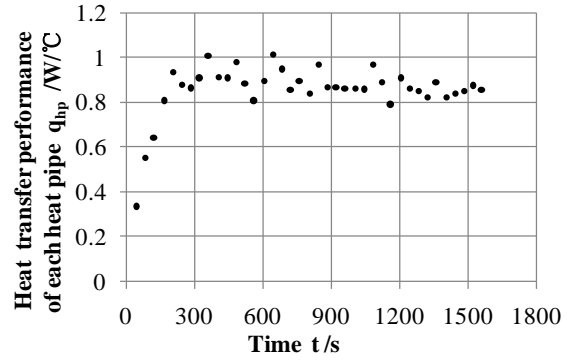
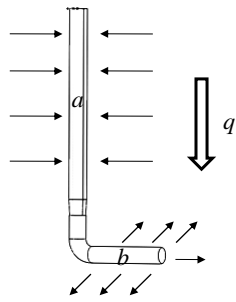
221 response tendency of the battery group and the coolant. As mentioned in the above
 222 calculation methodology, the model applied for the steady state is quasi-steady and it
 223 is not suitable for the dynamic process. So the initial calculated heat shown in Fig.3(b),
 224 which goes up to more than 200W, does not present the actual heat value. The average
 225 internal heat variation of the battery group and the coolant at the steady state is around
 226 119.4W and 83.6W respectively. Therefore according to equation (4), the specific heat
 227 of battery group can be gained, which about 1.24 kJ/kg°C. This result has also been
 228 verified by the following experiment based on the equation (1) and (2).



229 (a) Temperature response tendency (b) Internal heat variation response tendency
 230

231 Fig.3 Experimental response tendency

232 Heat transfer way of the heat pipe under this condition is shown as Fig 4. The top
 233 part *a* of the heat pipe absorbs heat from battery and the fluid inside takes the heat to
 234 the bottom part *b* to dissipate to the coolant. The fluid inside of the heat pipe
 235 evaporates at the top part, goes down to the bottom part by pressure, and goes up by
 236 capillary action after condensation. The heat transfer performance of each heat pipe
 237 (Fig.5) can be obtained by equation (3) and it shows that as the experiment goes to
 238 steady state the heat transfer performance of each heat pipe gets to a relative stable
 239 value, which is around 0.86W/°C.



240

241

Fig.4 Heat transfer way of the heat pipe

Fig.5 Heat transfer performance of each heat pipe

242

3.2.2 Cooling mode

243

On this mode the coolant is circulated by the pump with battery chiller cooling

244

and the battery group generates heat. The cooling capacity of the battery chiller is

245

adjusted by changing the opening degree of EXV3.

246

Fig.6 shows the temperature response of the battery cooling process. At the

247

beginning, the battery group and the coolant are on the same temperature condition.

248

As the cooling mode starts, the coolant average temperature inside of the battery

249

exchanger box decreases quickly. While the battery average temperature increases to a

250

higher value firstly and then begins to decrease with the coolant. It is worthy of

251

mention that as the battery average temperature increases to the highest point, the

252

temperature differences between the coolant and the battery group are all in the range

253

of 7~8°C under every experimental condition. This result shows that at the beginning

254

of this experimental mode, the battery begins to generate heat as it supplies power

255

while the HPHE does not start until the temperature difference goes up to 7~8°C.

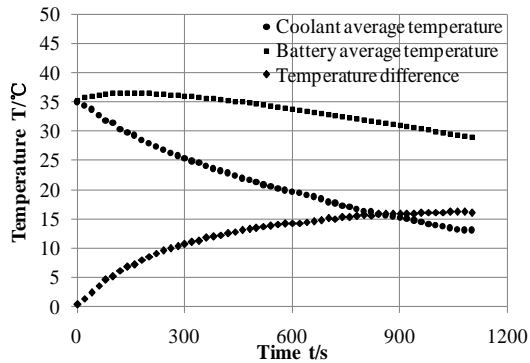
256

Therefore the battery group temperature will go up before the HPHE starts to transfer

257

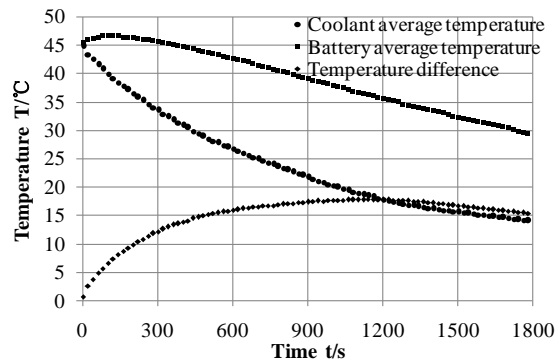
heat from the battery to the coolant. And finally the battery temperature decreases to

258 its suitable range. The battery cooling rate depends on the EXV3 opening degree.
 259 Under the conditions of 33% EXV3 opening degree, it takes about 1040s to be cooled
 260 from 35°C to 30°C, 1720 s from 45°C to 30°C. Under the conditions of 60% EXV3
 261 opening, it takes 600s from 35°C to 30°C, 1180s from 45°C to 30°C.



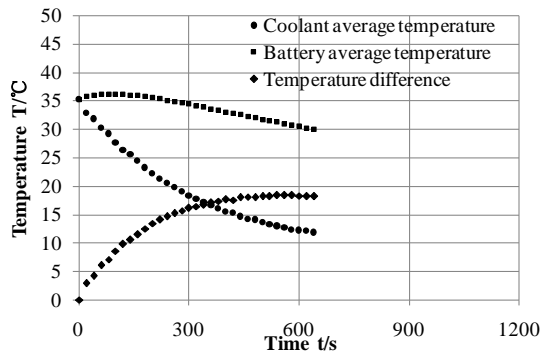
262

(a)35°C/33%



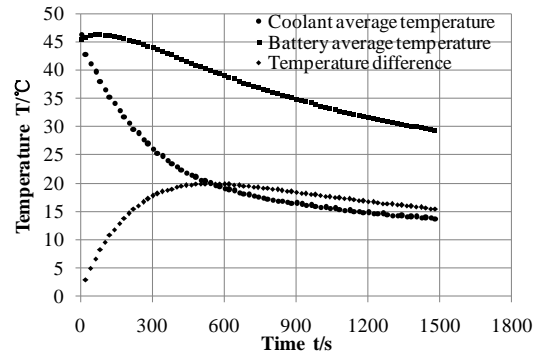
263

(b)45°C/33%



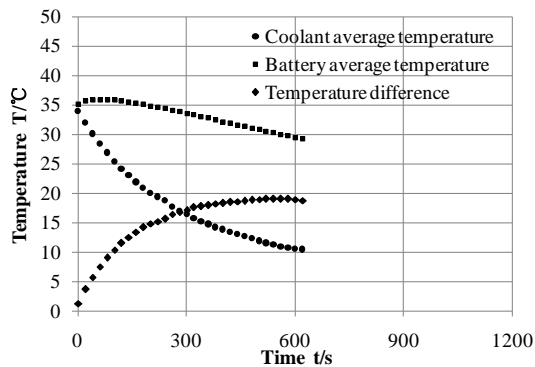
264

(c)35°C/60%



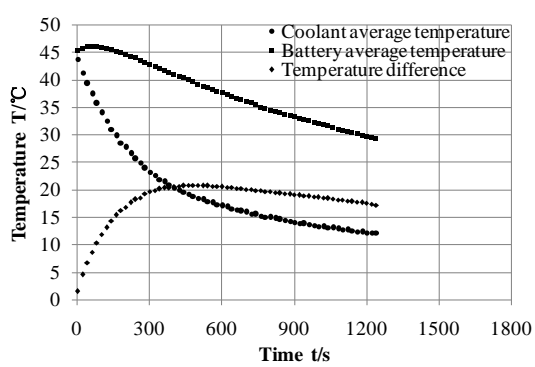
265

(d)45°C/60%



266

(e)35°C/100%



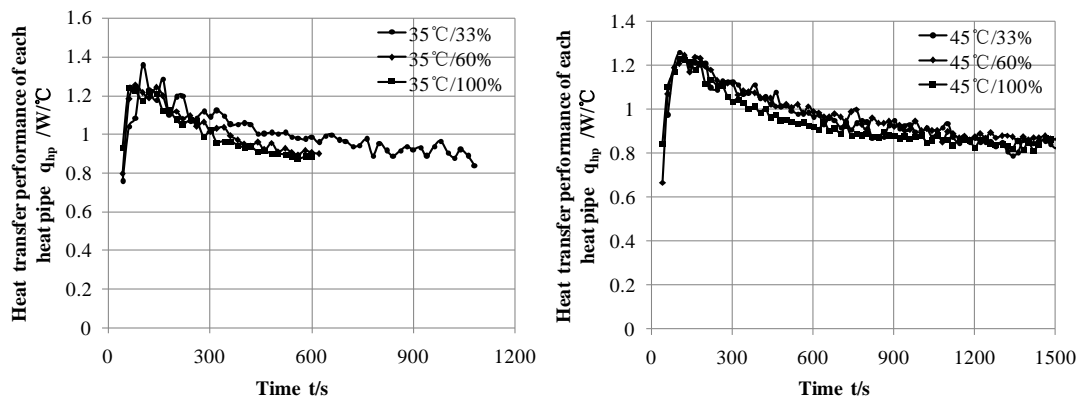
267

(f)45°C/100%

268

Fig.6 Temperature response tendency on cooling mode

269 Fig.7 shows the heat transfer performance of each heat pipe according to
 270 equations (1)~(3). Heat transfer way of the heat pipe under this condition is the same
 271 as fig 3. The results show that as the system runs to steady state the values of the heat
 272 pipe heat transfer performance on different working conditions go to be coincident,
 273 which is around 0.87 W/°C. This result is also fitting very well with the above
 274 experimental result. According to this result, the total heat transfer performance of the
 275 HPHE is easily to be estimated, so that the temperature difference between coolant
 276 and battery group can be determined accordingly in the real application.



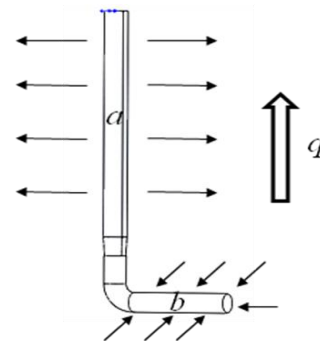
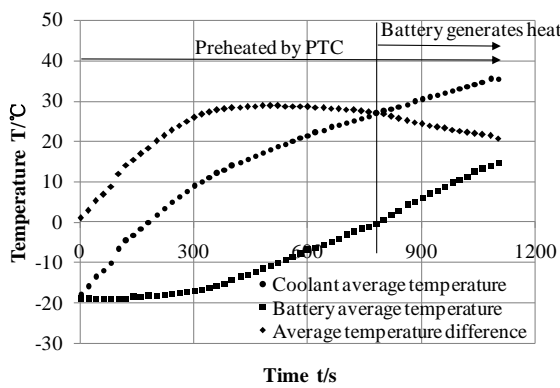
277
 278 Fig.7 Heat transfer performance of each heat pipe on cooling mode

279 3.2.3 Preheating mode

280 On this mode the coolant is circulated by the pump with PTC heating and the
 281 battery group begins to generate heat when its temperature gets to be higher than 0°C.

282 Fig.8 shows the temperature response of the battery preheating process under -20°C
 283 out-car temperature. The coolant average temperature increases quickly as the PTC
 284 heater is on. But the battery response temperature does not change at the first stage of
 285 200s until the coolant temperature goes up to be 2°C. After then it begins to increase

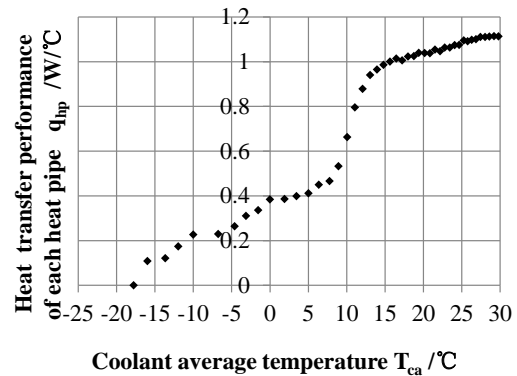
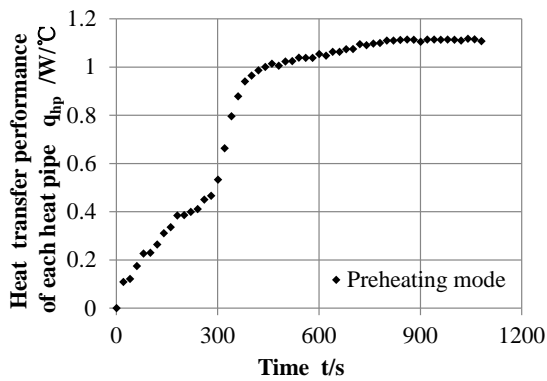
286 gradually with the increasing of the coolant temperature. This means the heat pipe
 287 also has a start condition on heating mode. The start temperature of its bottom
 288 evaporating terminal is about 2°C and the temperature difference between the
 289 evaporating terminal and condensing terminal under this condition is about 22°C. The
 290 battery begins to generate heat as its temperature gets higher than 0°C, so the increase
 291 rate of the battery temperature is getting higher after 0°C.



292

293 Fig.8 Temperature response on preheating mode

Fig.9 Heat transfer way of the heat pipe



294

295

Fig.10 Heat transfer performance on preheating mode

296 Fig 9 shows the heat transfer way of the heat pipe under preheating mode. The
 297 bottom part *b* of the heat pipe absorbs heat from coolant and the top part *a* preheats
 298 the battery. The fluid inside of the heat pipe evaporates at the bottom part, goes up to
 299 the top part by the central route of the pipe with the heat and gets down by the inside

300 wall of the pipe after condensation. Fig.10 shows the heat transfer performance of
301 each heat pipe on preheating mode. At first the heat transfer performance increases
302 gradually at a relative low level with the increasing of the temperature difference. As
303 the coolant temperature goes up to be higher than 8°C, the heat transfer performance
304 jumps up quickly to a higher value, and then increases slowly to a relative stable value,
305 which is about 1.11W/°C. This result verifies that the coolant temperature has
306 important effect on the heat transfer performance of the HPHE because the
307 evaporating and condensing process of the fluid inside of the heat pipe depends on the
308 temperatures of its two terminals. Meanwhile, compare to the heat transfer
309 performance of the heat pipe on cooling mode, that on heating mode is higher. This is
310 because on heating mode the heat pipes can take advantage of the gravity role to get
311 better heat transfer performance. The HPHE designed for this experimental bench can
312 be on a good heat transfer performance when the coolant average temperature is
313 higher than 15°C.

314 **4. Conclusion**

315 According to the above experimental research on an integrated thermal
316 management system for EV, the cooling and heating performance of heat pump
317 system and heat transfer performance of HPHE are investigated. The research results
318 show that the presented system works well as an effective thermal management
319 method for EV. The main conclusions go as following:

320 (1) The system cooling performance shows that the additional parallel branch of
321 battery chiller is a good way to solve the battery group cooling problem, which can
322 supply about 20% additional cooling capacity without input power increase. The
323 cooling capacity distribution of each branch under different working conditions can
324 be optimized by adjusting the expansion valve.

325 (2) The system heating performance under extremely cold condition shows that
326 although the heating COP under -20°C in-car temperature is higher than that under
327 20°C , the compression efficiency of the scroll compressor is much lower because the
328 motor efficiency of scroll compressor drops rapidly under lower load conditions. So
329 improving the heating performance under high temperature difference condition is
330 still an important future work for EV.

331 (3) The specific heat of the battery group is tested about $1.24\text{ kJ/kg}^{\circ}\text{C}$. On cooling
332 mode, there is a delay for the HPHE to start heat transfer and the temperature
333 difference for the HPHE to start between its two terminals is about $7\sim 8^{\circ}\text{C}$. The heat
334 pipe heat transfer performance on different cooling working conditions is around 0.87
335 $\text{W}/^{\circ}\text{C}$.

336 (4) On preheating mode, the HPHE also has a necessary start condition. The start
337 temperature of the bottom evaporating terminal is about 2°C and the temperature
338 difference between the two terminals is about 22°C . The coolant temperature has
339 important effect on the heat transfer performance of HPHE. As the coolant
340 temperature goes up to be higher than 8°C , the heat transfer performance jumps up

341 quickly to a higher value, and then increases slowly to a relative stable value, which is
342 about 1.11W/°C. The heat transfer performance of the heat pipe on preheating mode,
343 is higher than that on heating mode because it can take advantage of the gravity role.

344 (5) The research results show that the heat transfer performance of HPHE can meet
345 the demand of battery temperature control on different working conditions. According
346 to the heat transfer performance of the HPHE and specific heat of the battery group,
347 the design parameters of the coolant system can be determined based on the
348 calculation methodology in the real applications.

349 **5. Acknowledgements**

350 We would like to thank the support by the Natural Science Foundation of China
351 (No. 51576203) and the External Cooperation Program of BIC, Chinese Academy of
352 Sciences (No. 1A1111KYSB20130032)

353 **6. References**

354 [1] Chen Y, Evans JW. Heat transfer phenomena in lithium/ polymer- electrolyte
355 batteries for electric vehicle application. Journal of the Electrochemical Society. 1993;
356 140:6.

357 [2] Song L, Evans JW. The thermal stability of lithium polymer batteries. Journal of
358 Electrochemical Society.1998; 145: 2327-2334.

359 [3] Sato N. Thermal behavior analysis of lithium-ion batteries for electric and hybrid
360 vehicles. Journal of Power Sources, 2001; 99:70-77.

-
- 361 [4] Khateeb SA, Amiruddin S, et al. Thermal management of Li-ion battery with
362 phase change material for electric scooter: experiment validation. *Journal of Power*
363 *Sources*, 2005; 142:345-353.
- 364 [5] Pesaran AA. Battery thermal models for hybrid vehicle simulations. *Journal of*
365 *Power Sources*. 2002; 110: 377-382.
- 366 [6] BEHR. *Thermal Management for Hybrid Vehicles*. Technical Press Day. 2009.
- 367 [7] Mahamud R, Park C. Reciprocating air flow for Li-ion battery thermal
368 management to improve temperature uniformity. *Journal of Power Sources*. 2011;
369 196(13):5685–96.
- 370 [8] Wu MS, Liu KH, Wang YY, Wan CC. Heat dissipation design for lithium-ion
371 batteries. *Journal of Power Sources* 2002;109(1):160
- 372 [9] Al Hallaj S, Selman JR. A novel thermal management system for electric vehicle
373 batteries using phase-change material. *Journal of Electrochemical Society*. 2000;
374 147(9):3231.
- 375 [10] Ling Z, Chen J, et al. Experimental and numerical investigation of the application
376 of phase change materials in a simulative power batteries thermal management system.
377 *Applied Energy*. 2014;121:104-113.
- 378 [11] Wang T, Tseng KJ, et al. Thermal investigation of lithium-ion battery module
379 with different cell arrangement structures and forced air-cooling strategies. *Applied*
380 *Energy*. 2014;134:229-238.
- 381 [12] Zhao JT, Rao ZH, Li YM. Thermal performance of mini-channel liquid cooled

382 cylinder based battery thermal management for cylindrical lithium-ion power battery.
383 Energy Conversion and Management.2015;103: 157–165

384 [13] Khateeb SA, Amiruddin S. et al. Thermal management of Li-ion battery with
385 phase change material for electric scooter: experiment validation. Journal of Power
386 Sources, 2005;142:345-353.

387 [14] Kim US, Shin CB, Kim CS. Modeling for the scale-up of a lithium-ion polymer
388 battery. Journal of Power Sources. 2009; 189:841-846.

389 [15] Yang X, Yan YY, Mullen D. Recent developments of lightweight, high
390 performance heat pipes. Applied Thermal Engineering. 2012; 33-34:1-14.

391 [16] Esen M, Esen H. Experimental investigation of a two-phase closed
392 thermosyphon solar water heater. Solar Energy. 2005; 79(5):459-468.

393 [17] Remeli MF, Date A, Ding LC, et al. Experimental investigation of combined heat
394 recovery and power generation using a heat pipe assisted thermoelectric generator
395 system. Energy Conversion and Management. 2016; 111: 147-157.

396 [18] Rao Z, W SH. Experimental investigation on thermal management of electric
397 vehicle batterywith heat pipe. Energy Conversion and Management. 2013; 65:92-97.

398 [19] Wang Q, Zou HM, Yan. YY, et al. Experimental investigation on EV battery
399 cooling and heating by heat pipes. Applied Thermal Engineering. 2015, 88:54-60.

400 [20] Suzuki T, Ishii K. Air conditioning system for electric vehicle. SAE technical
401 paper no. 960688.

402 [21] Hosoz M, Direk M. Performance evaluation of an integrated automotive air
403 conditioning and heat pump system. Energy Conversion and Management. 2006; 47:

404 545-559.

405 [22] Direk M, Hosoz M, et al. Experimental performance of an R134a automobile
406 heat pump system coupled to the passenger compartment. World renewable energy
407 congress 2011. Sweden.

408 [23] Qi ZG. Advances on air conditioning and heat pump system in electric vehicles –
409 A review. Renewable and Sustainable Energy Reviews. 2014;38: 754-764.

410 [24] Qin F, Zou HM, Tian CQ, et al. Experimental investigation on heating
411 performance of heat pump for electric vehicles at -20 °C ambient temperature. Energy
412 Conversion and Management.2015;102: 39-49.

413 [25] Qin F, Zou HM, Tian CQ, et al. Experimental investigation and theoretical
414 analysis of heat pump systems with two different injection portholes compressors for
415 electric vehicles. Applied Energy. 2016, In Press.